

***NIR, MWIR and LWIR Quantum Well
Infrared Photodetector using Interband
and Intersubband Transitions***



Fabio Durante P. Alves (ITA – Brazil)



G. Karunasiri and N. Hanson (NPS – USA)



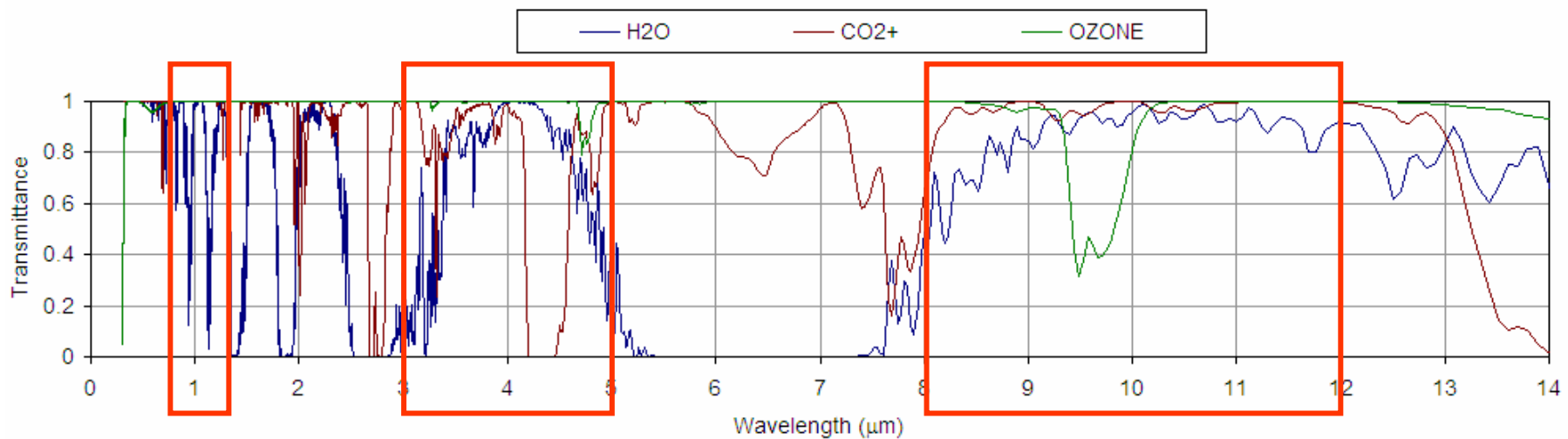
***M. Byloos, H. C. Liu, A. Bezingier
and M. Buchanan (NRC – Canada)***

Motivation

$\lambda \sim 8 - 12 \mu m$

$\lambda \sim 3 - 5 \mu m$

$\lambda \sim 0.8 - 1.2 \mu m$

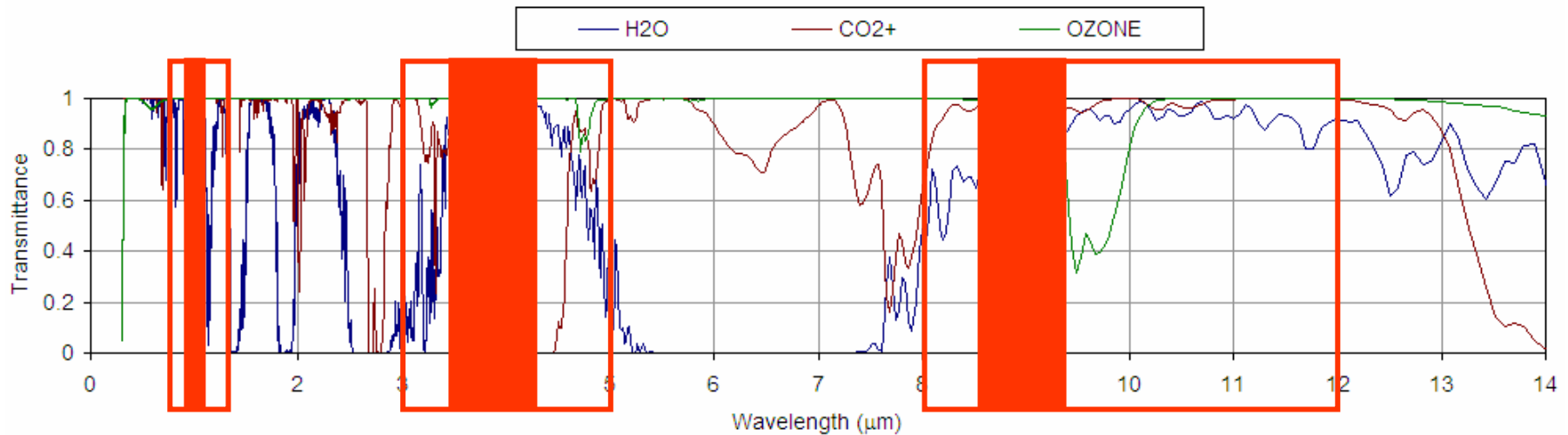


Motivation

LWIR - $\Delta\lambda \sim 1 \mu\text{m}$

MWIR - $\Delta\lambda \sim 1 \mu\text{m}$

NIR - $\Delta\lambda \sim 0.1 \mu\text{m}$



Purpose

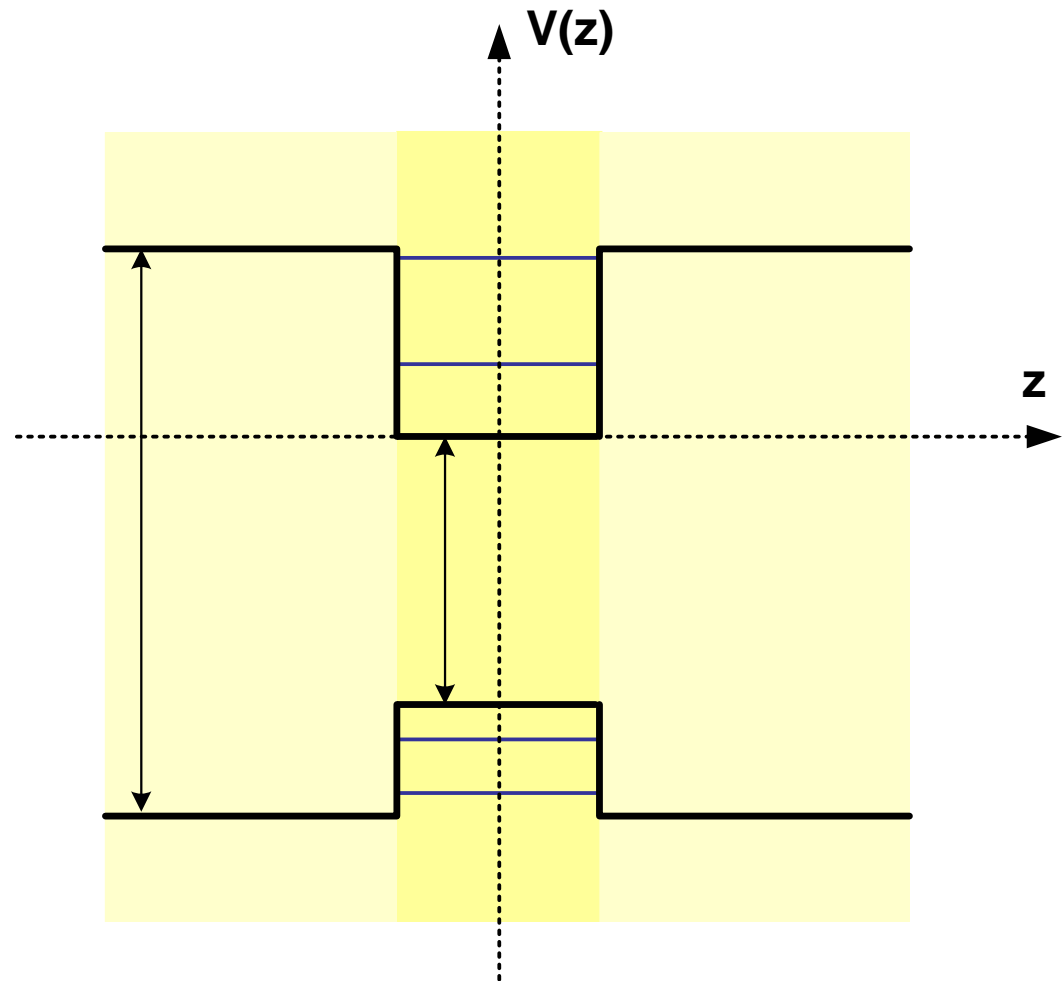
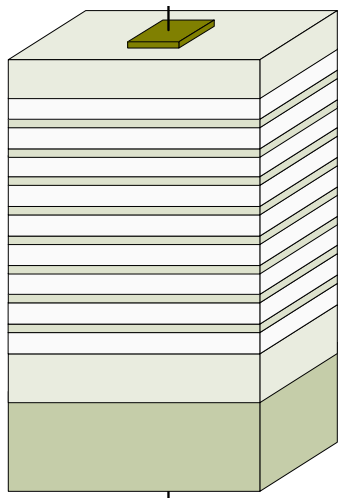
To investigate the feasibility of a QWIP capable to detect **simultaneously** 3 different IR bands within the wavelengths intervals of 0.8 - 1.2 μm , 3.0 - 5.0 μm and 8.0 - 12.0 μm .

Outline

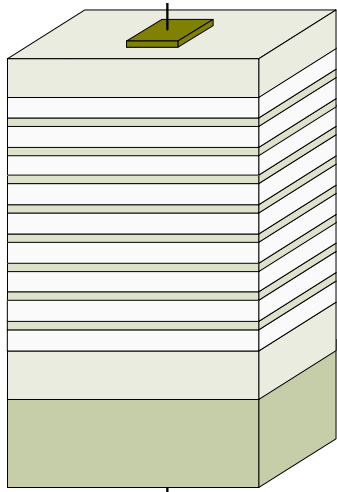
- QWIP Design
- Experimental Results
- Future work

Design and Modeling Considerations

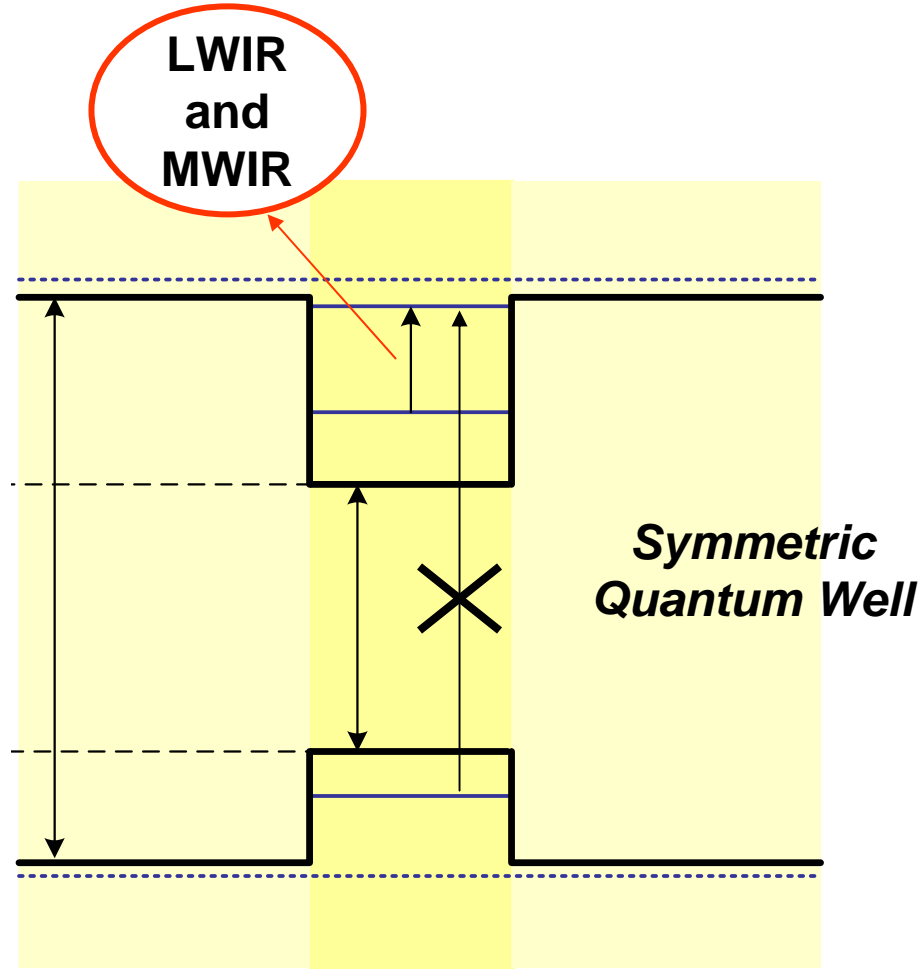
Quantum Wells



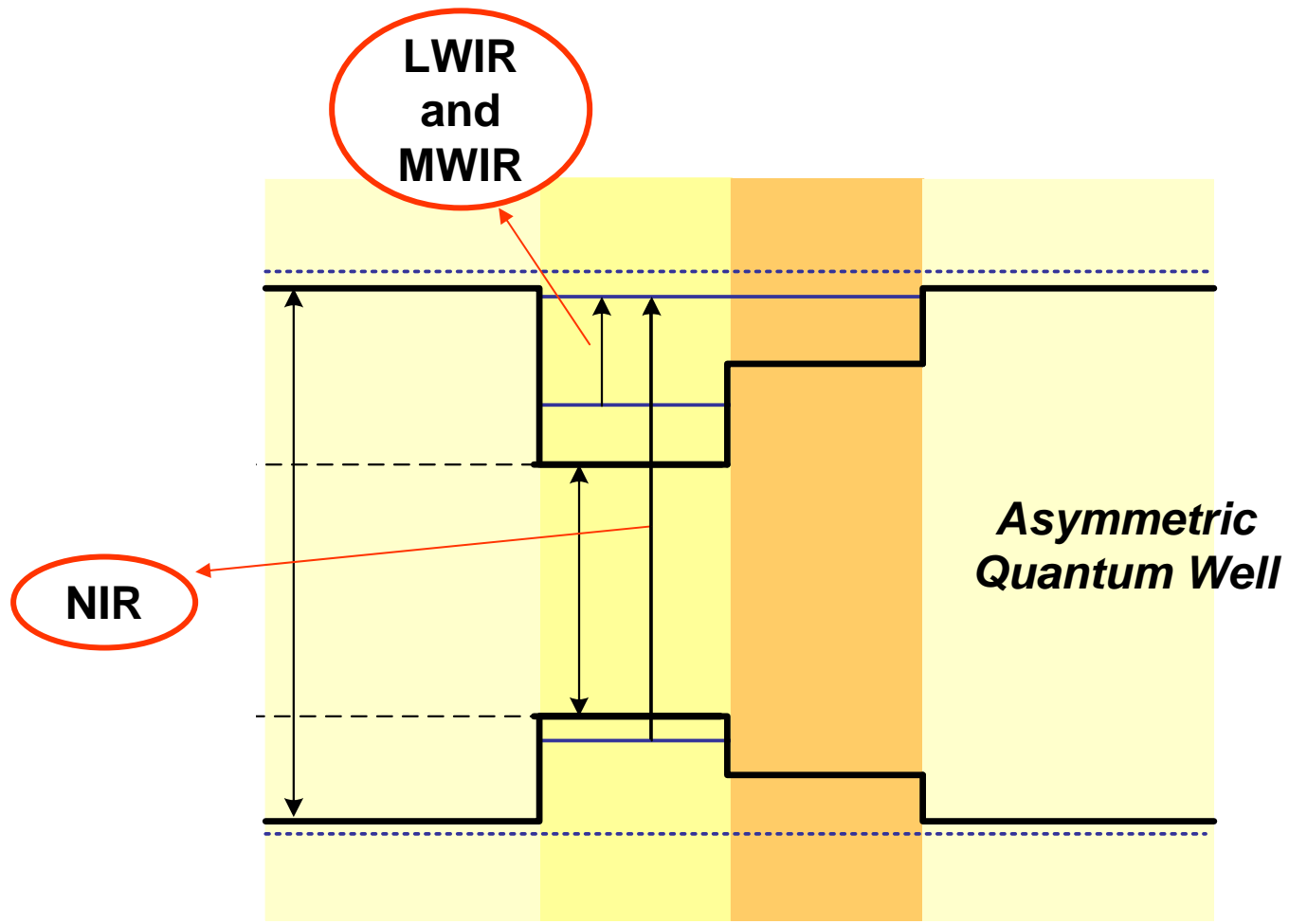
MWIR and LWIR



*Incident IR
radiation*



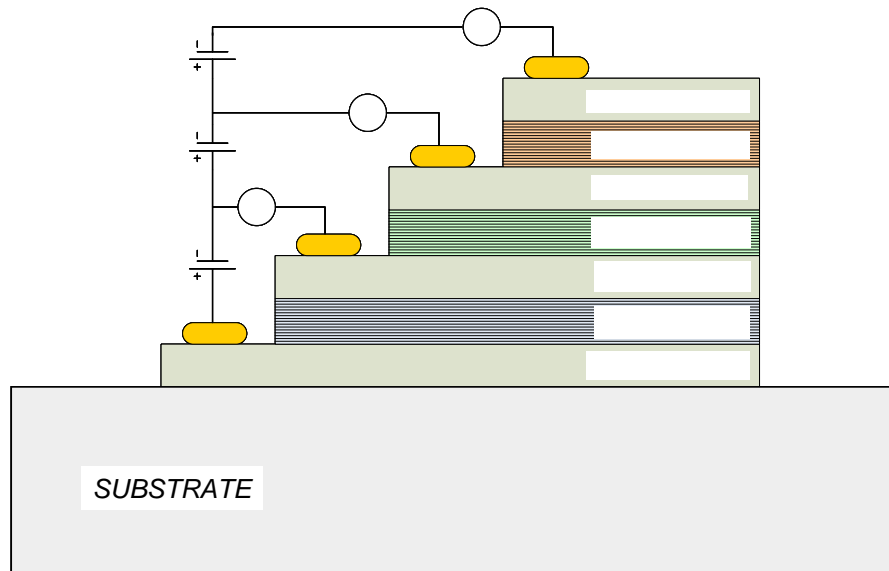
Semiconductor Heterostructure



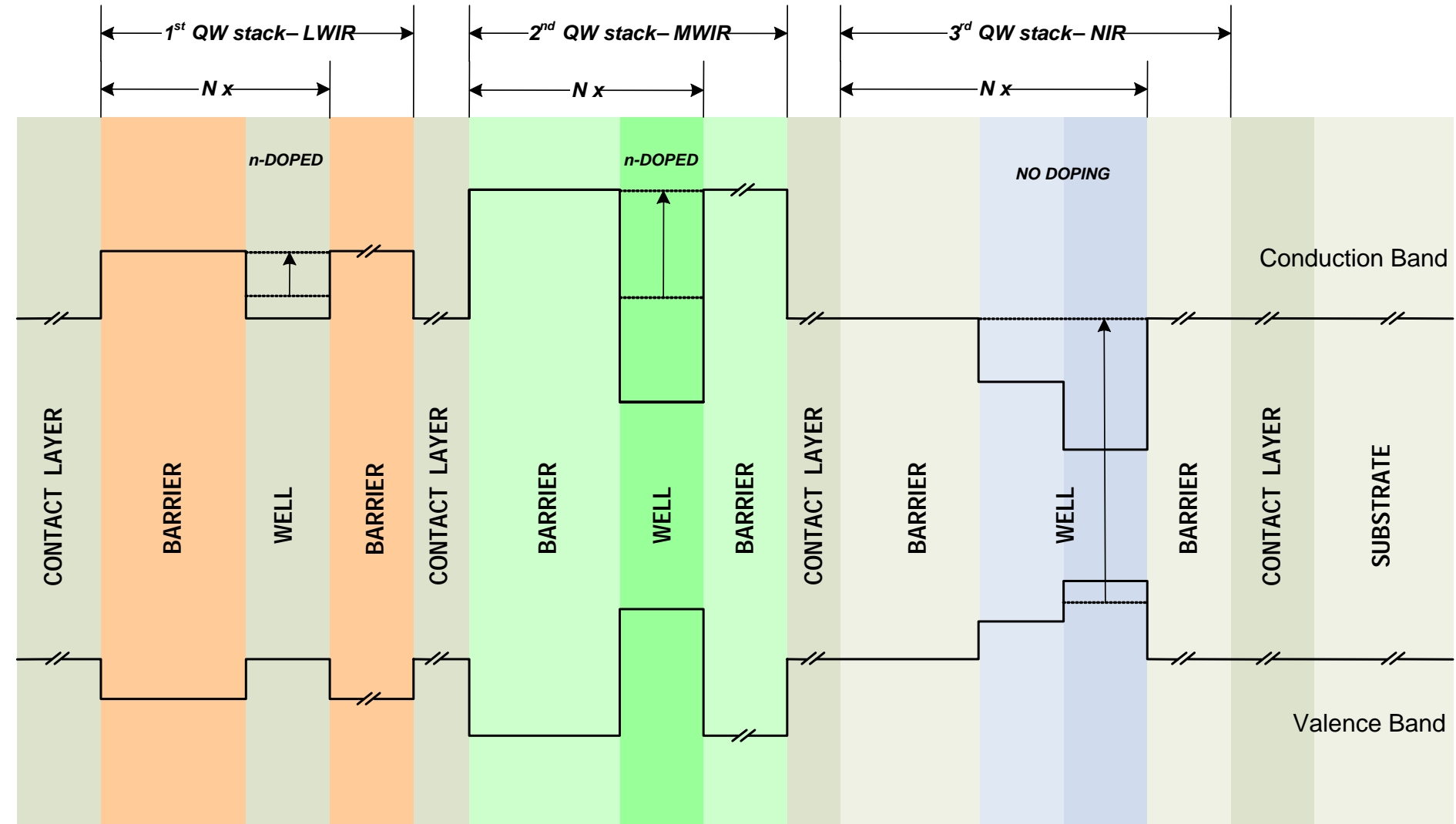
Semiconductor Heterostructure

Design and Modeling Considerations

To have the capability to detect simultaneously three different IR bands, with independent readouts, we employed a configuration with three different stacks of quantum wells formed by alloys of GaAs, AlGaAs and InGaAs, separated by heavily doped GaAs contact layers.



Design and Modeling Considerations



Design and Modeling Considerations

The barriers were made large to have uncoupled quantum wells in all stacks;

The quantum wells for each stack were computed independently;

The electron wavefunctions in the heterostructure were computed using the effective mass approximation for the one-dimensional potential profile along the growth direction;

The band non-parabolicity effects were considered;

The strain due to the difference in lattice constants between GaAs or AlGaAs and InGaAs crystal layers was not taken into account;

For the valence band, the heavy and light hole bands were represented using average negative effective masses, m_{hh} and m_{lh} , respectively;

One-dimensional time independent Schrödinger's Equation

$$-\frac{\hbar^2}{2} \frac{\partial}{\partial z} \frac{1}{m^*(z)} \frac{\partial}{\partial z} \psi(z) + V(z)\psi(z) = E\psi(z)$$

One-dimensional time independent Schrödinger's Equation

$$-\frac{\hbar^2}{2} \frac{\partial}{\partial z} \frac{1}{m^*(z)} \frac{\partial}{\partial z} \psi(z) + V(z)\psi(z) = E\psi(z)$$

Potential Profile

$$V_b(z) = -qFz$$

External electric field potential

Poisson equation

$$\nabla^2 V_\rho = -\frac{\rho}{\epsilon}$$

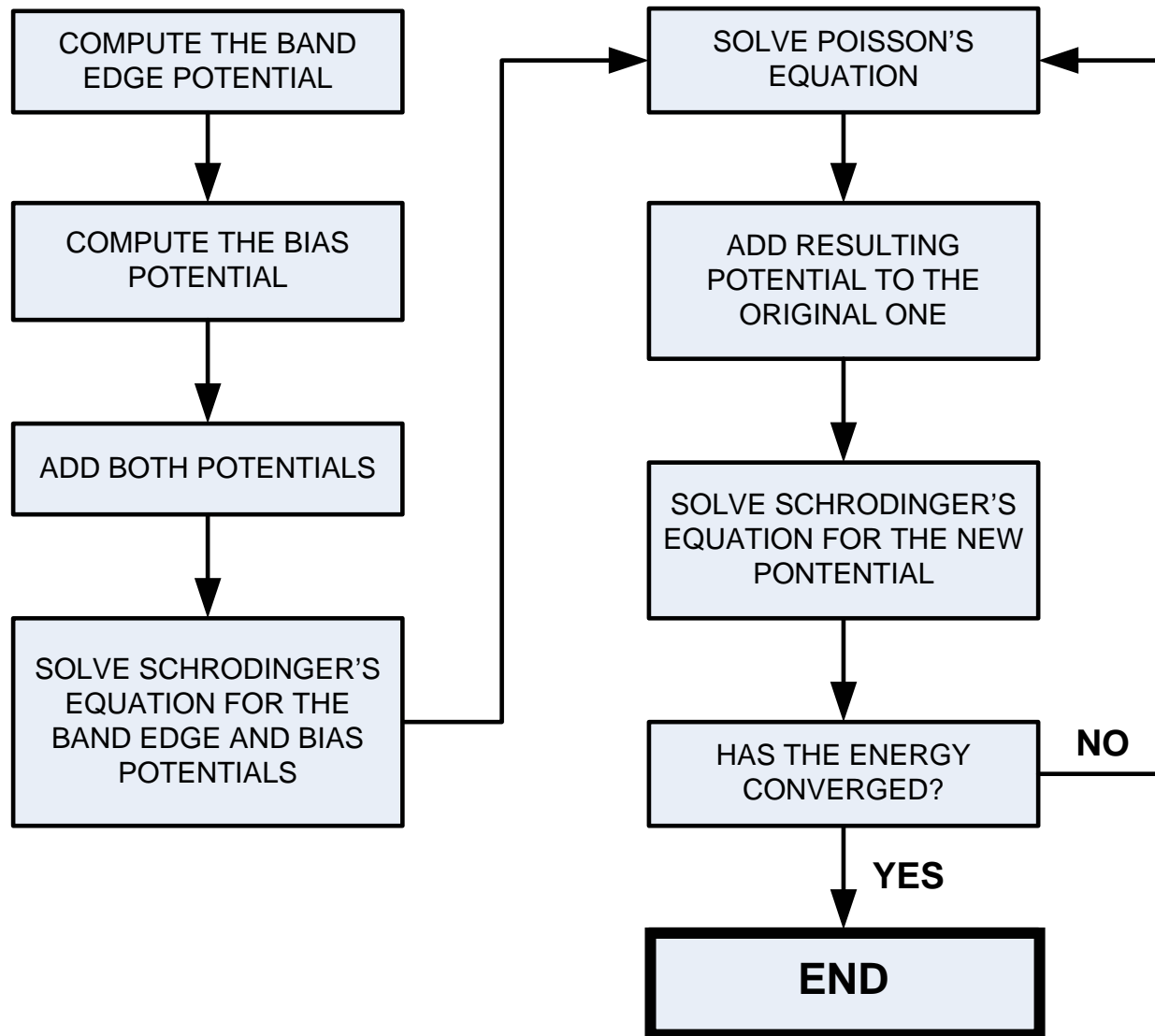
Charge distribution potential

$$V(z) = V_e(z) + V_b(z) + V_\rho(z)$$

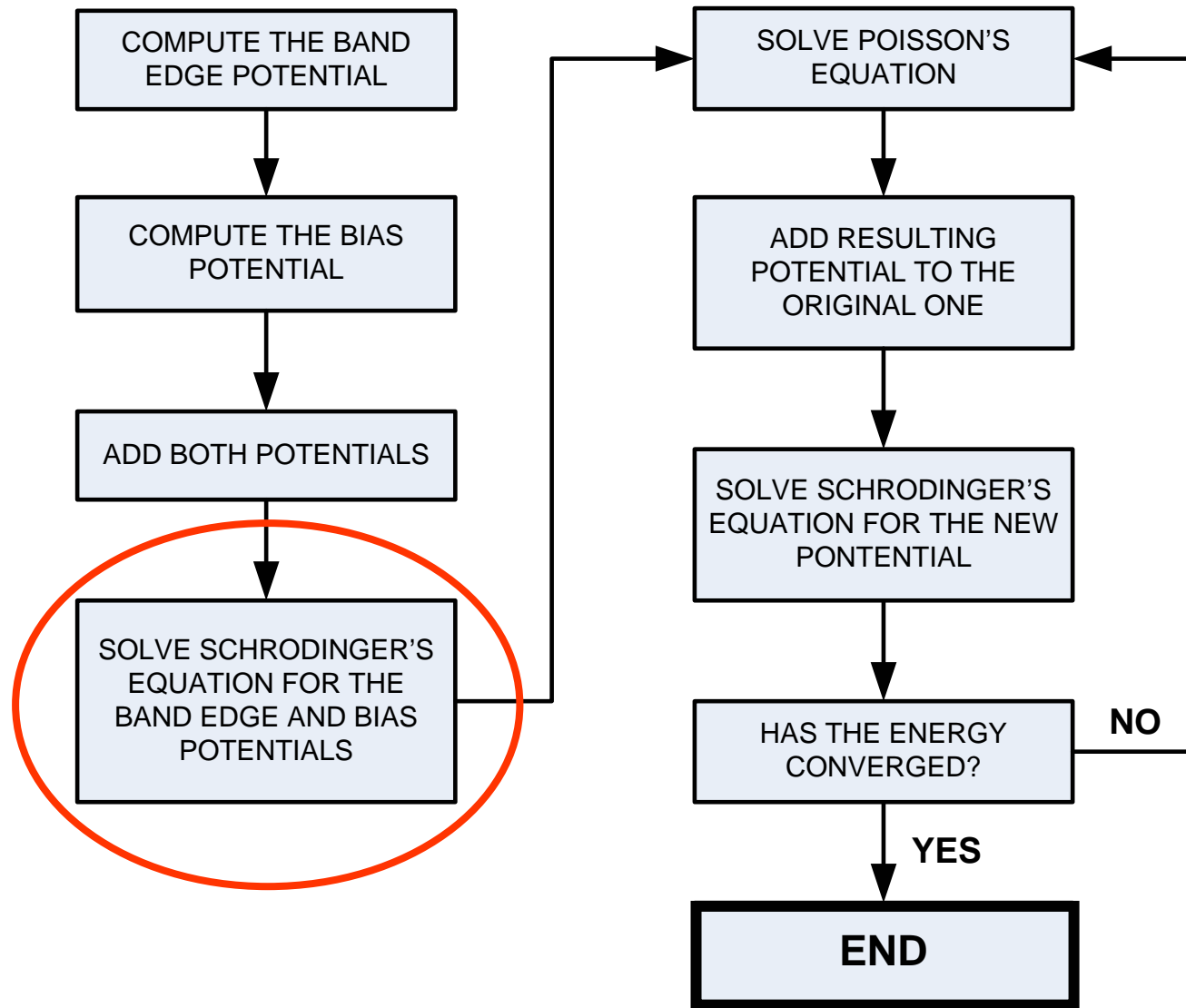
Bandedge potential

$$V_b(z) = (E_{g,n+1} - E_{g,n}) \delta_{n,n+1}$$

Self-Consistent Schrödinger-Poisson Solution



Self-Consistent Schrödinger-Poisson Solution



Shooting Method

$$\frac{\psi(z + \delta z)}{m^*(z + \delta z/2)} = \left\{ \frac{2(\delta z)^2}{\hbar^2} [V(z) - E] + \frac{1}{m^*(z + \delta z/2)} \right. \\ \left. + \frac{1}{m^*(z - \delta z/2)} \right\} \psi(z) - \frac{\psi(z - \delta z)}{m^*(z - \delta z/2)}$$

- Knowing two values of the wavefunction,

$$\begin{array}{c} \psi(z - \delta z) \\ | \\ \psi(z) \end{array}$$

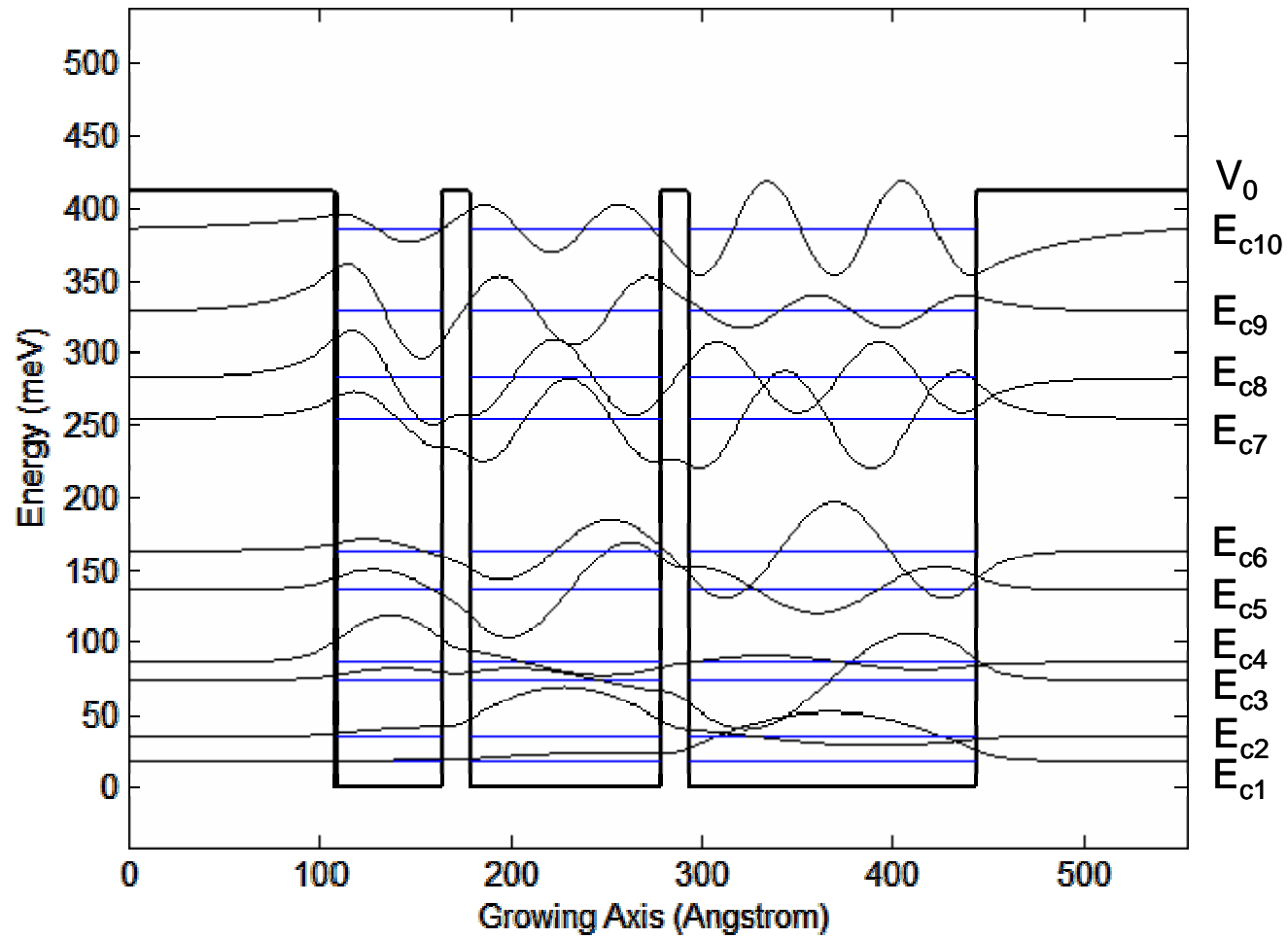
- The third point can be predicted $\longrightarrow \psi(z + \delta z)$

Using the new point together with its predecessor, a fourth point can be calculated and so on. Hence the wavefunction can be deduced for any particular energy value.

Shooting Method

- Multiple layer structures
 - Handle arbitrary potential profiles
 - Efficient to compute biased structures
 - Suitable to be used in self-consistent solutions
-
- Convergence problems with wide barriers
 - Computationally expensive

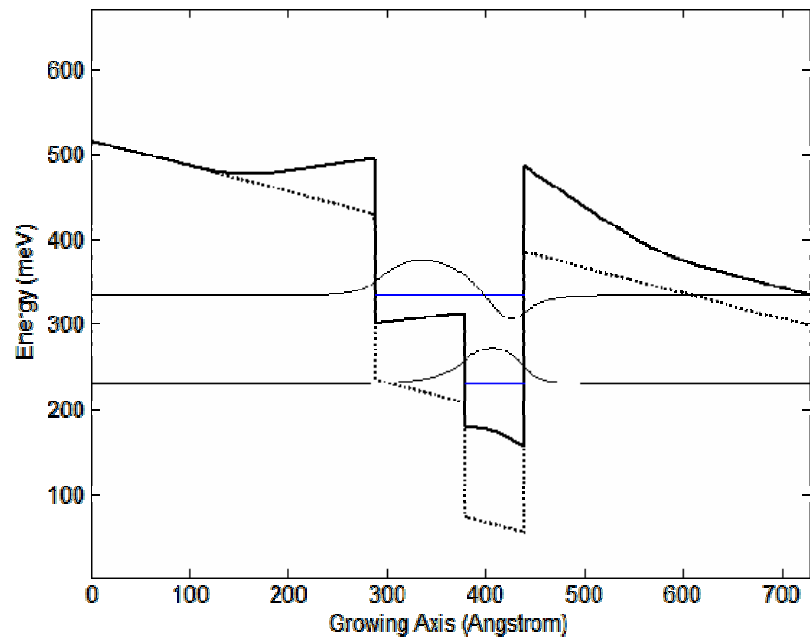
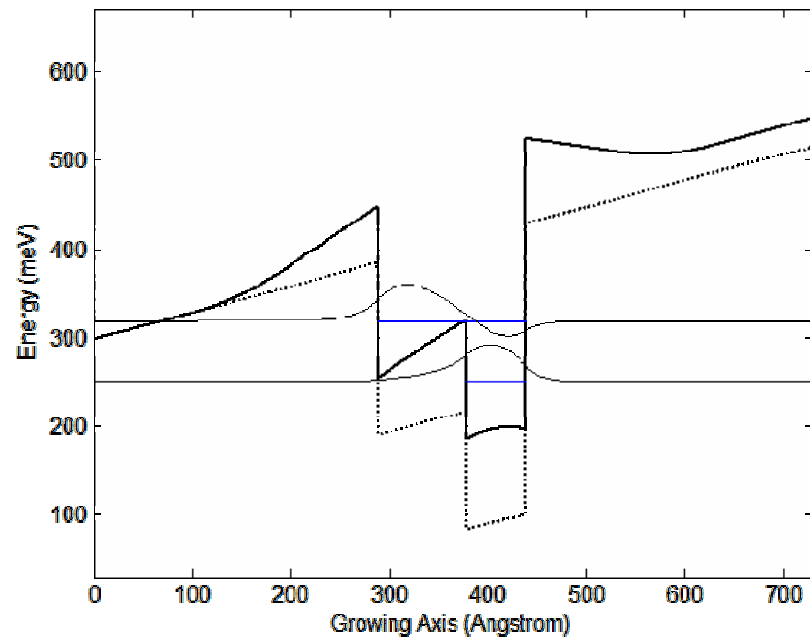
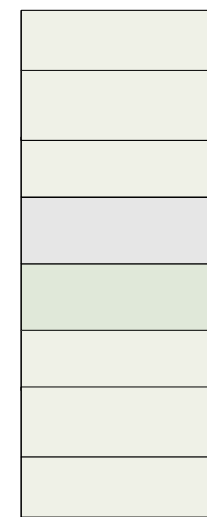
Shooting Method



Clayton L. Workman, "Intersubband Transitions in Strained InGaAs Quantum Well for Multi-color Infrared Detector Applications," PhD Thesis, University of Arkansas, 2000.

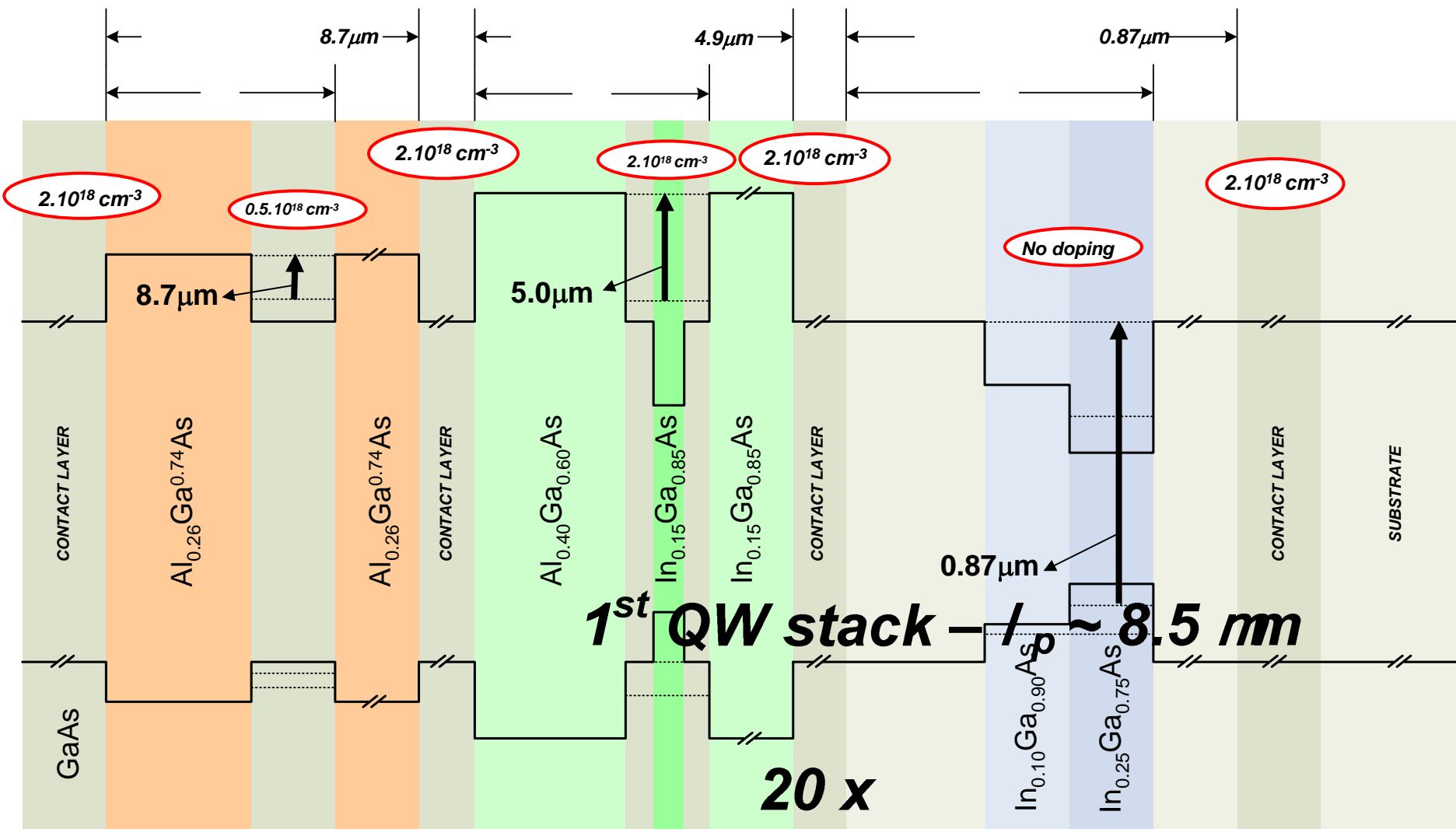
Al Ga_{0.53}As 100 Å

Self-Consistent Schrödinger-Poisson Solution

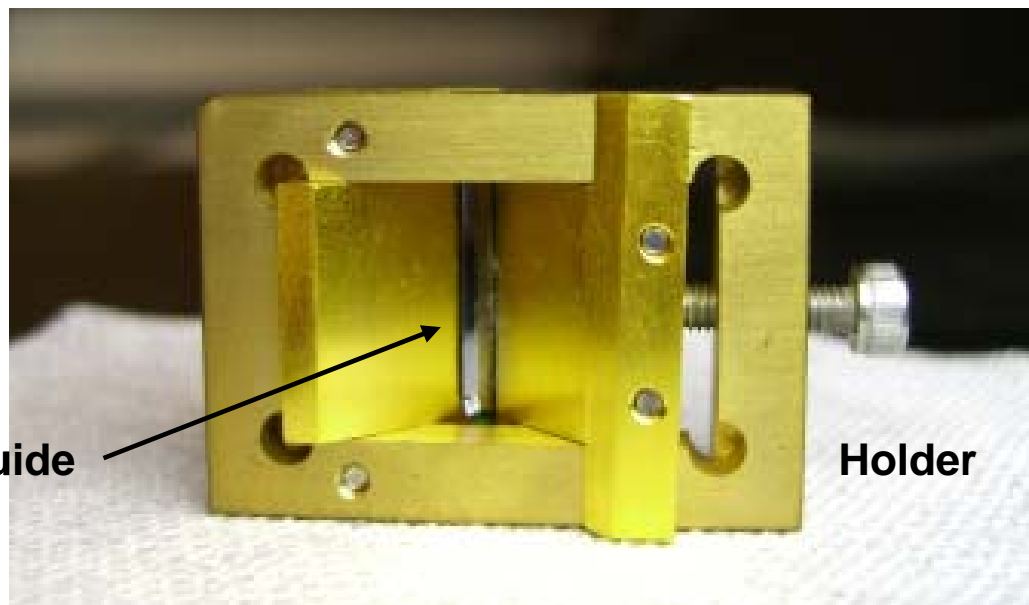
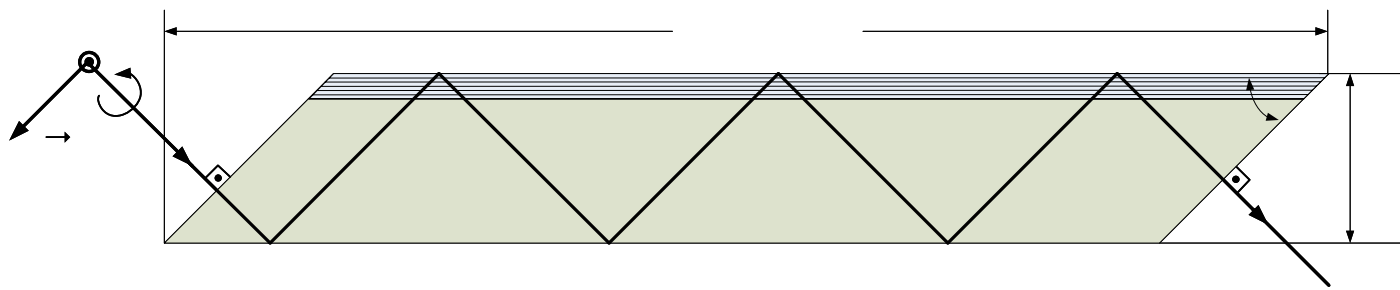


Wafer Structure

Strained InGaAs/GaAs/AlGaAs



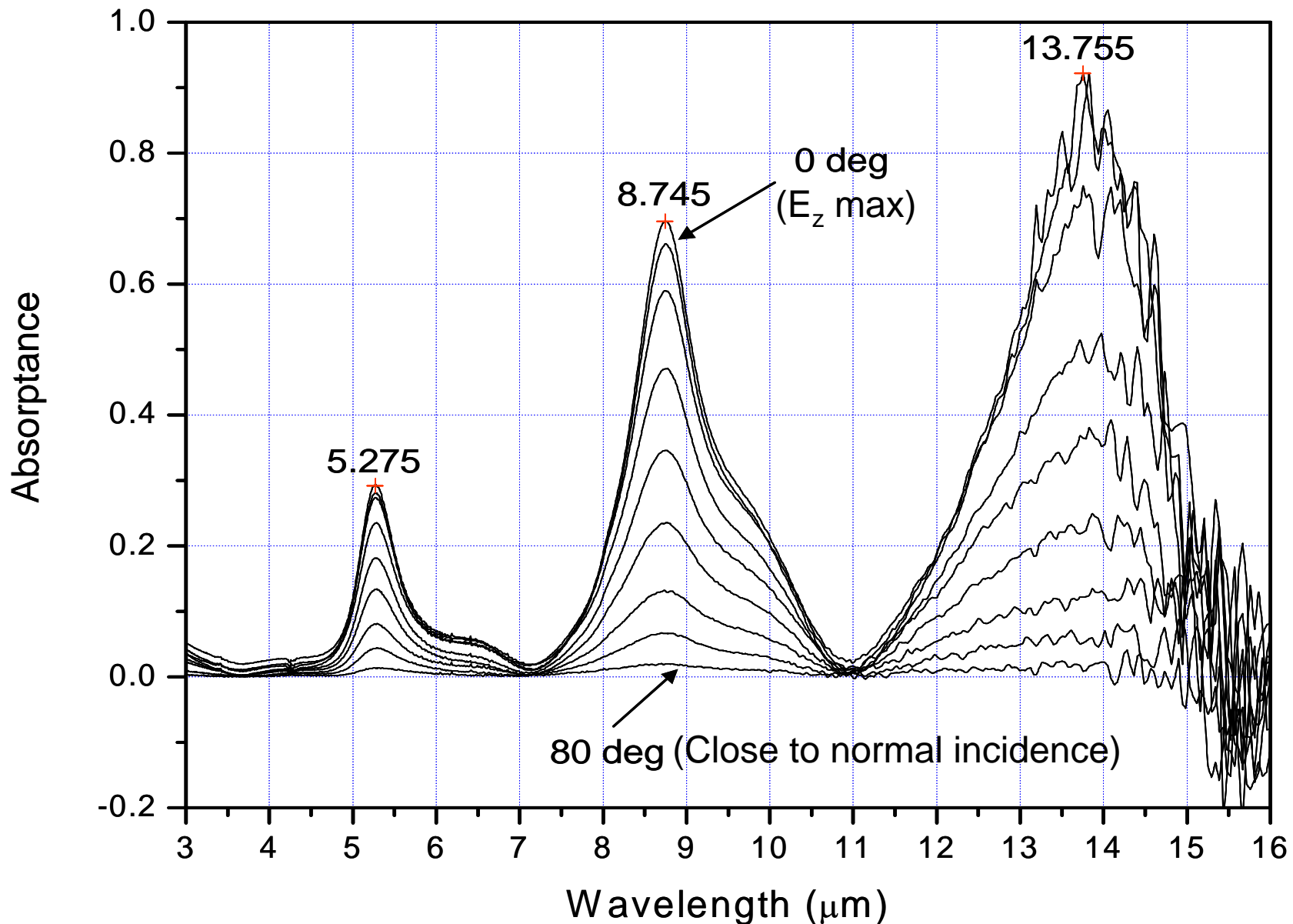
Experimental Results



Waveguide configuration

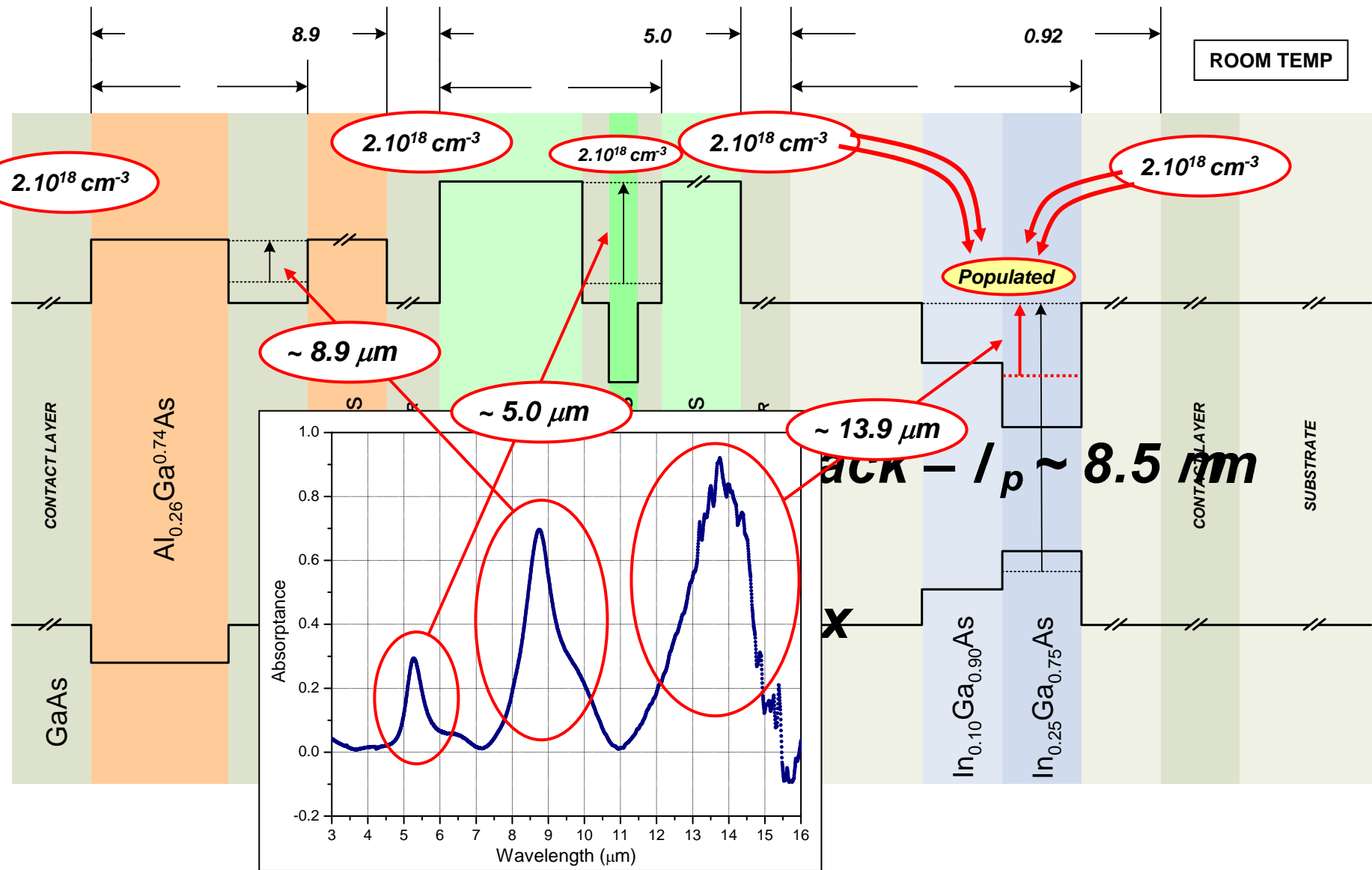
Experimental Results

Intersubband Absorption Measurements



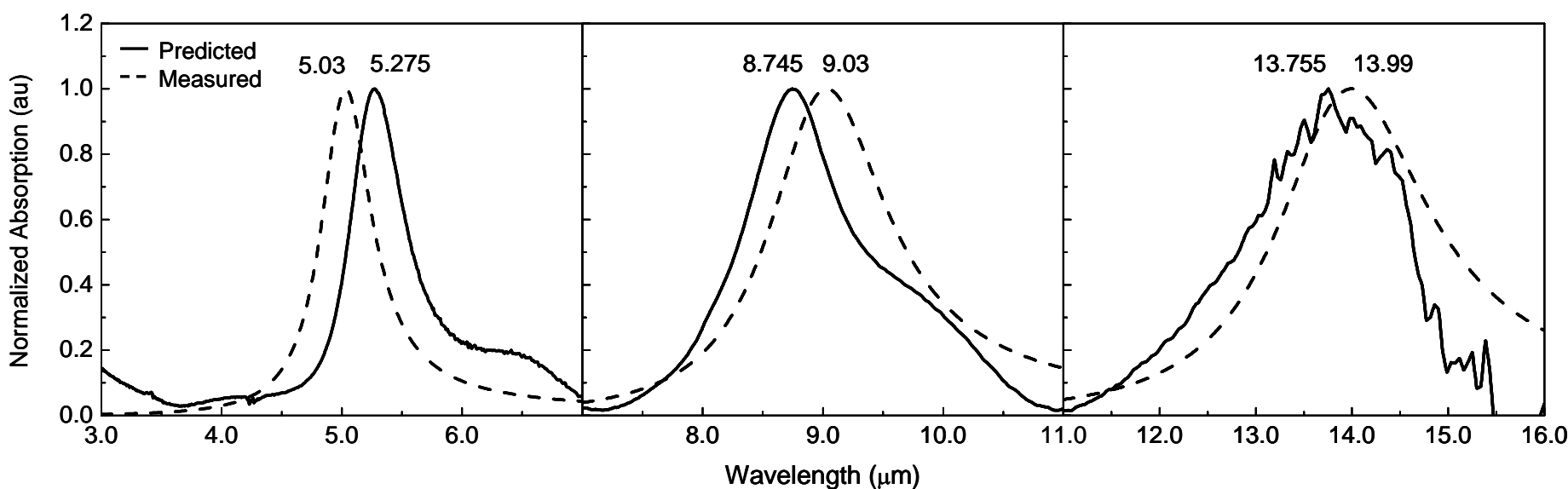
Experimental Results

Intersubband Absorption Measurements

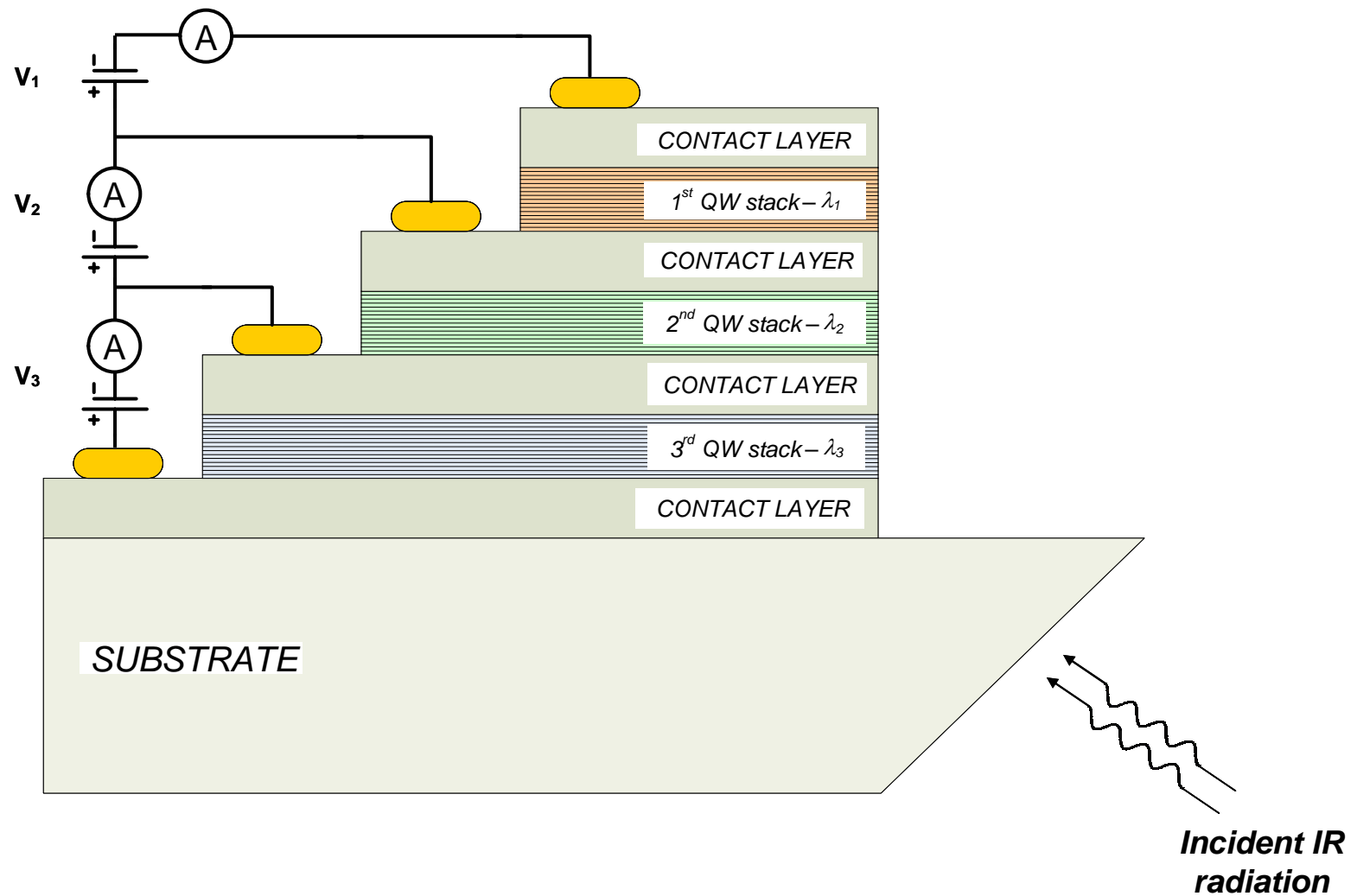


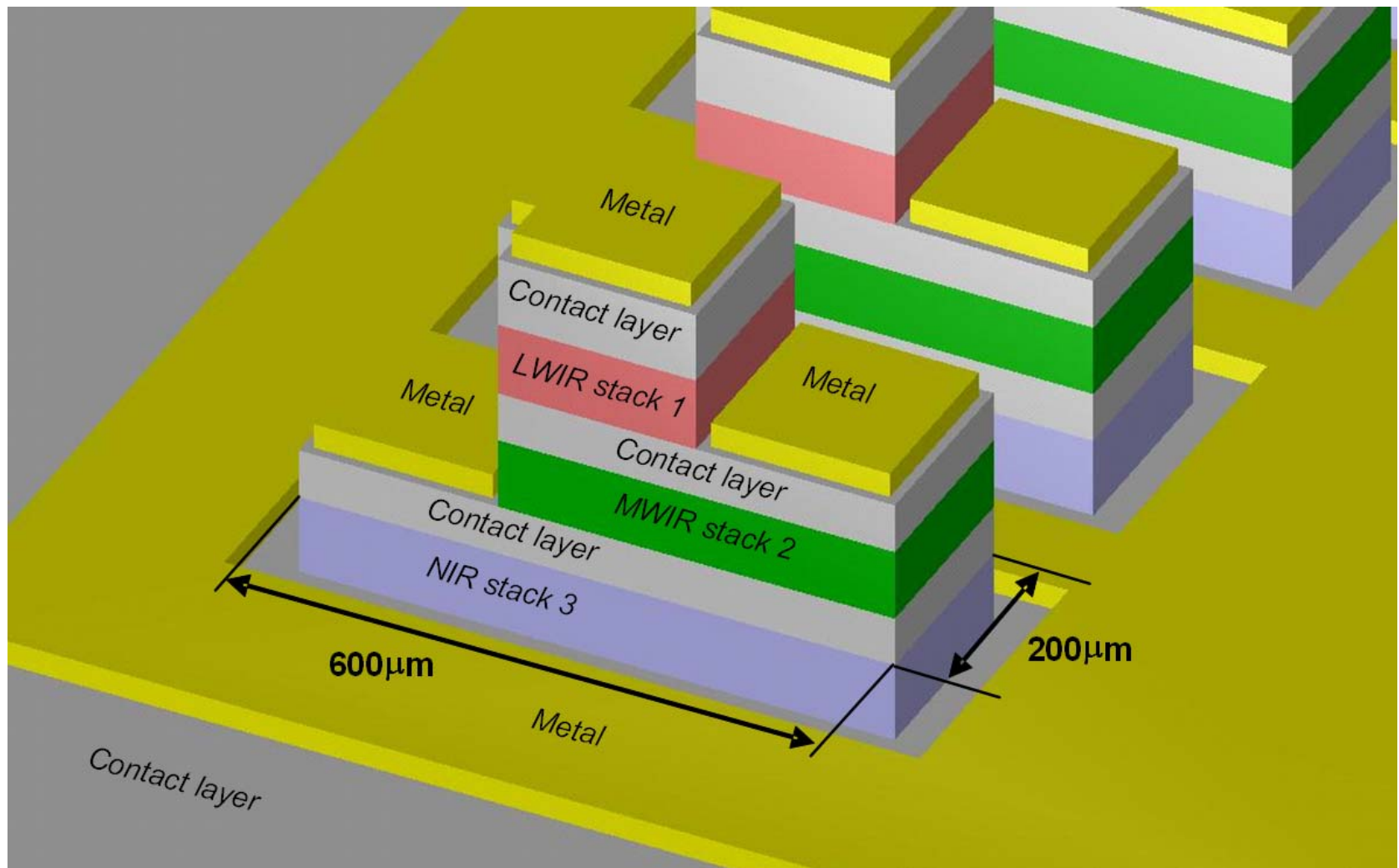
Experimental Results

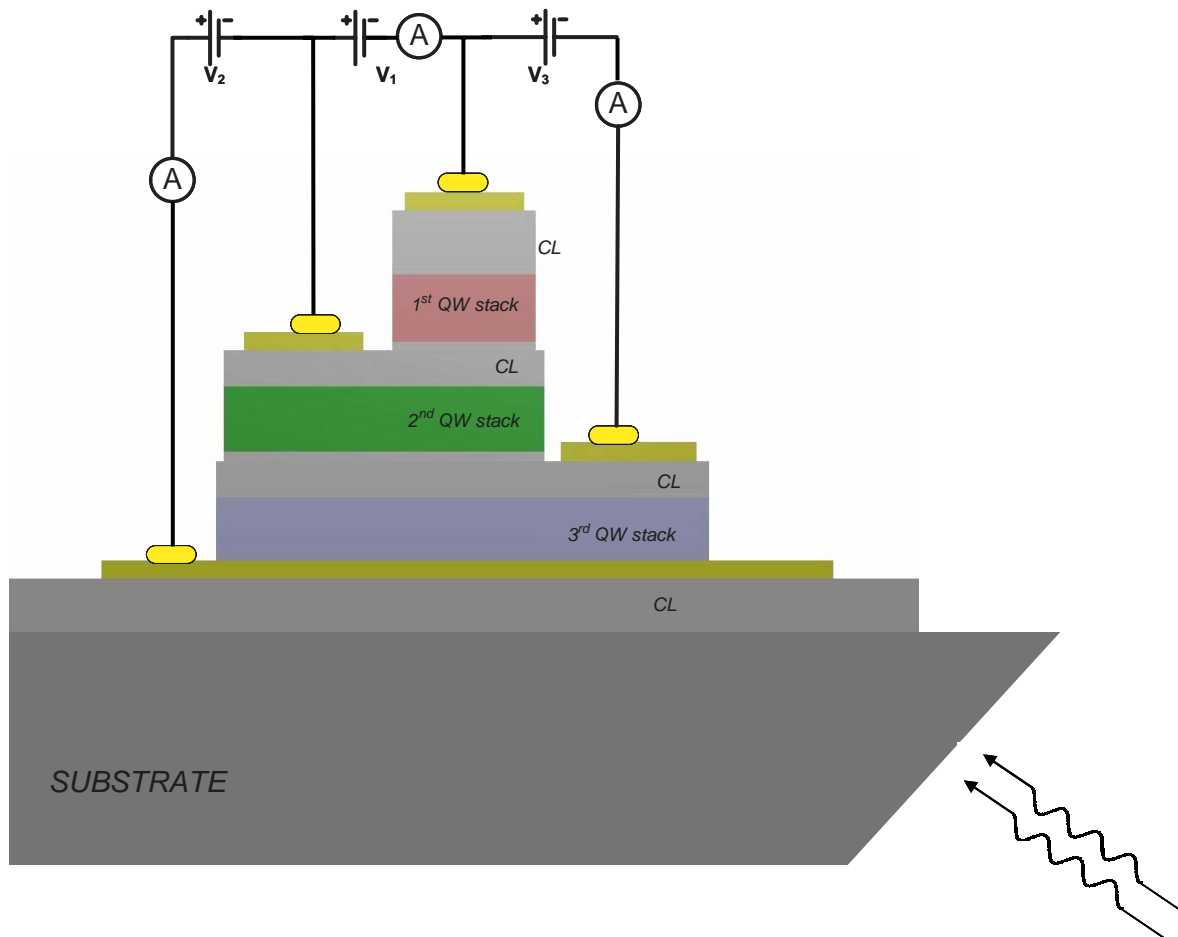
Absorption Measurements

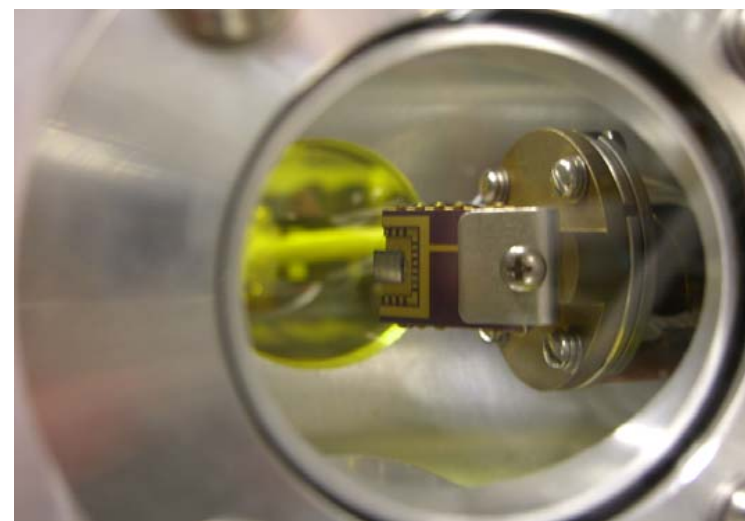
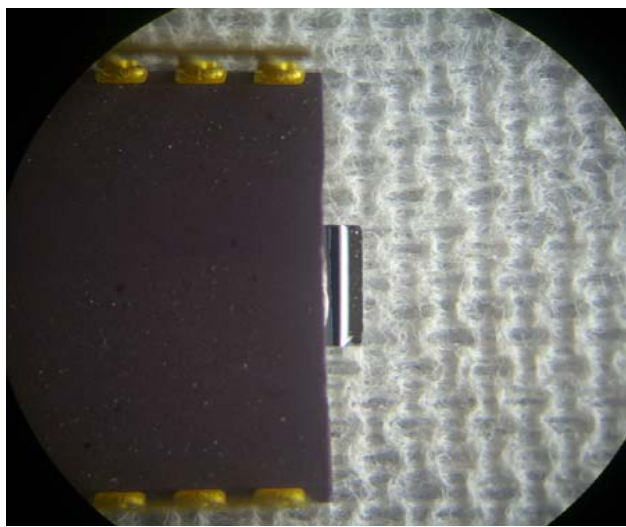
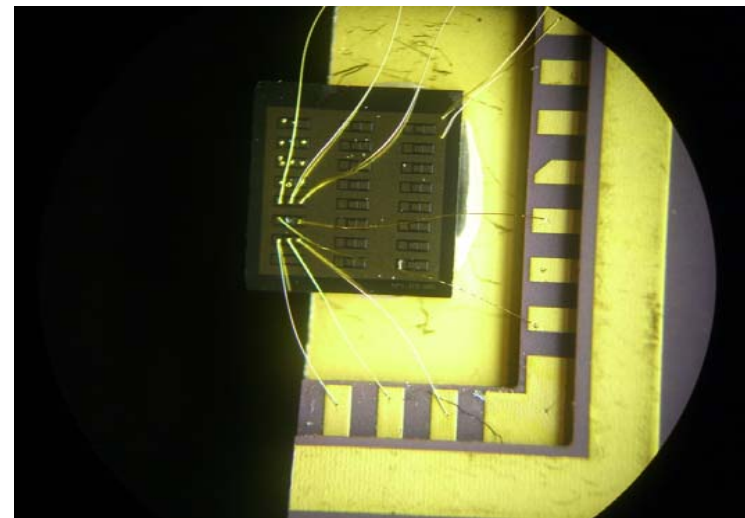
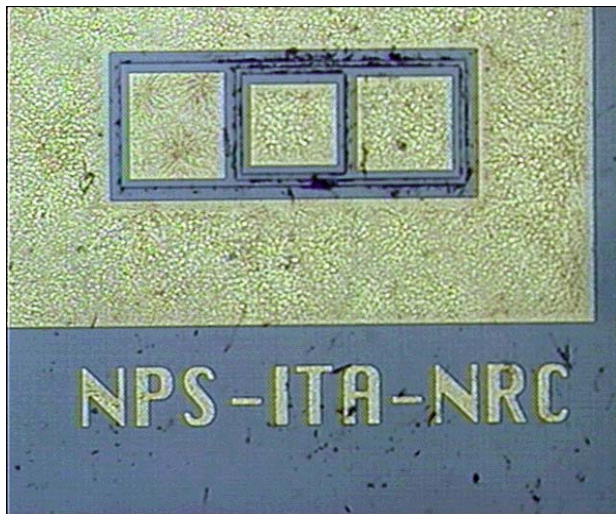


Devices Configuration



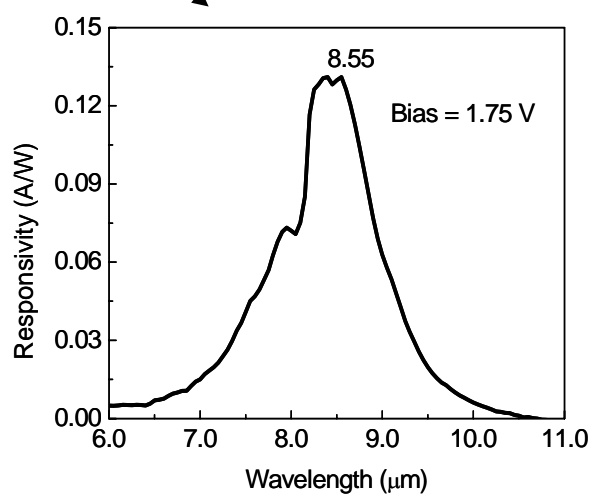
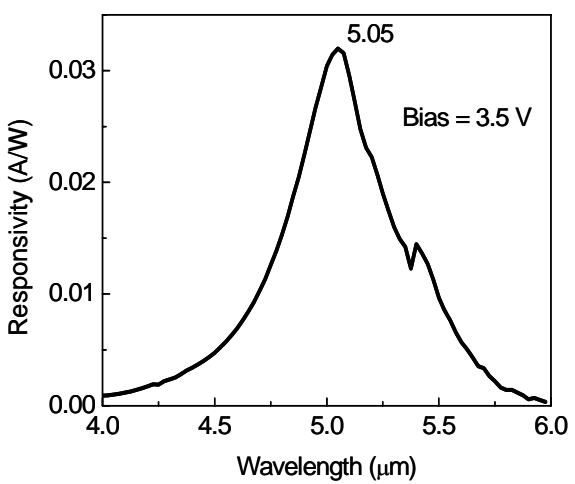
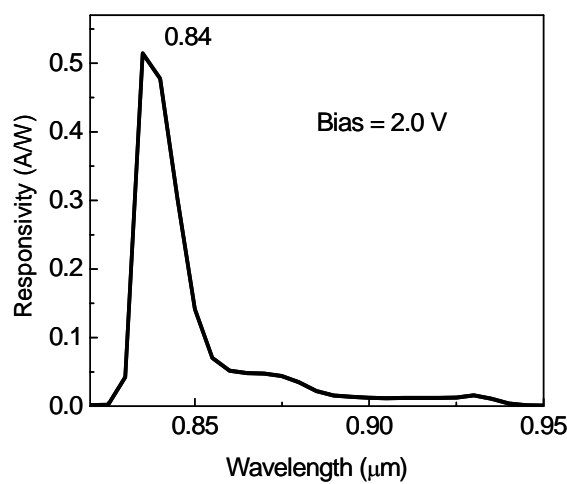
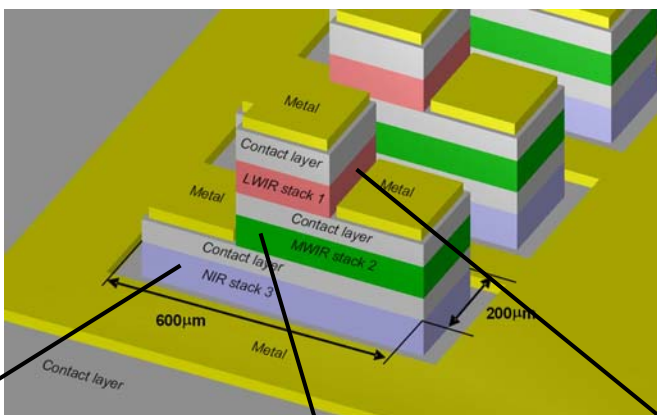


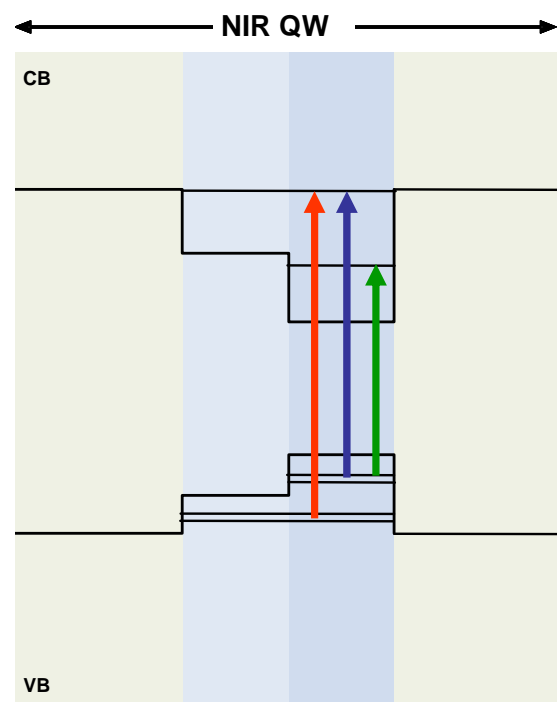
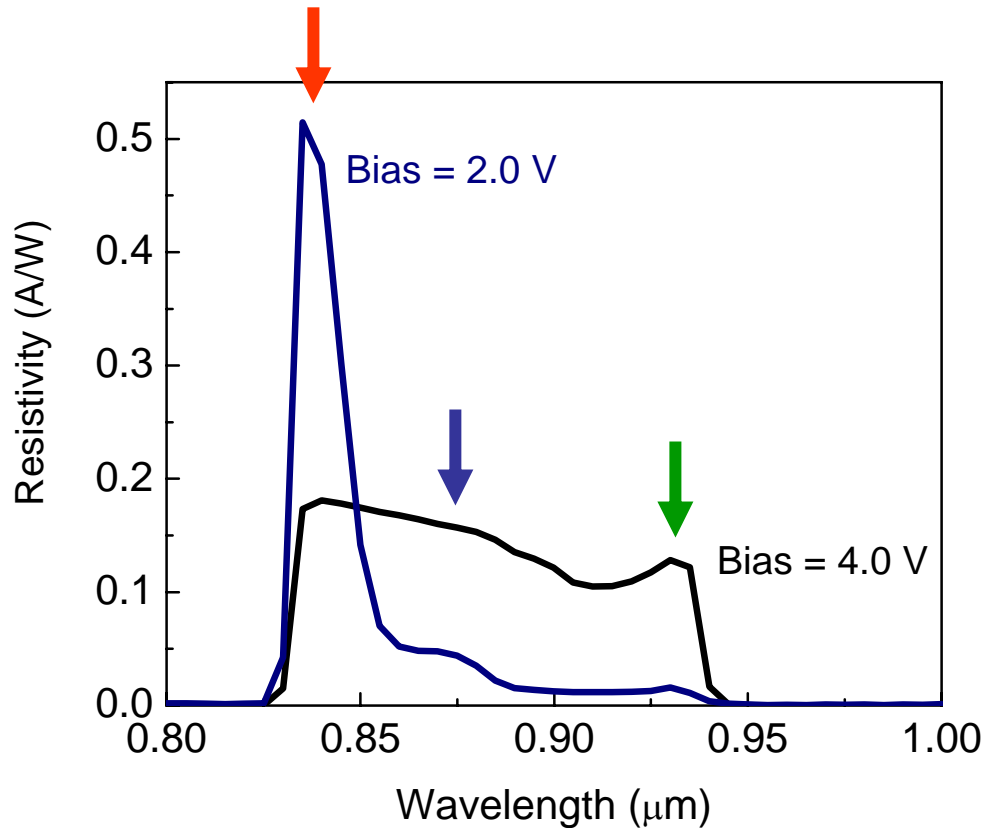




Experimental Results

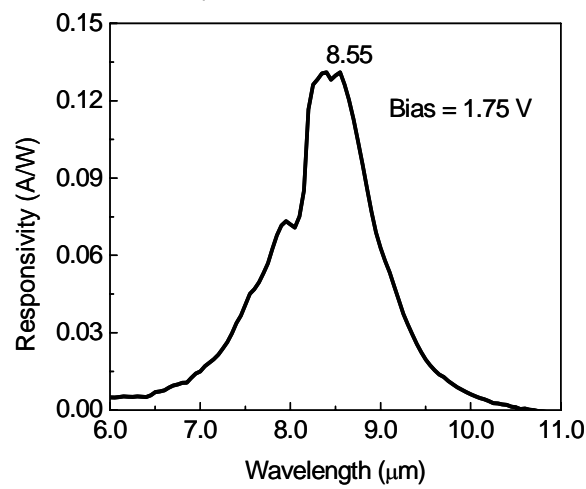
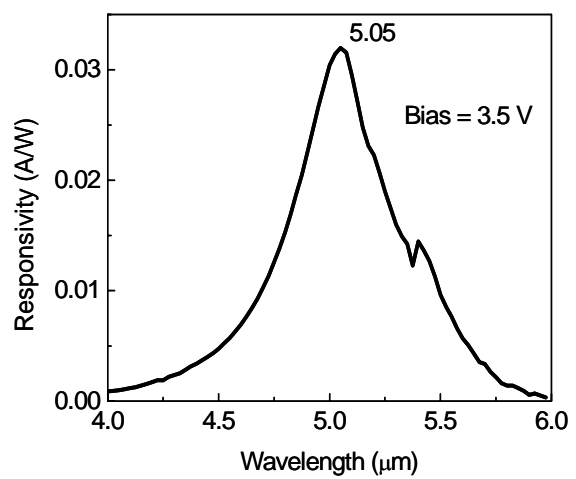
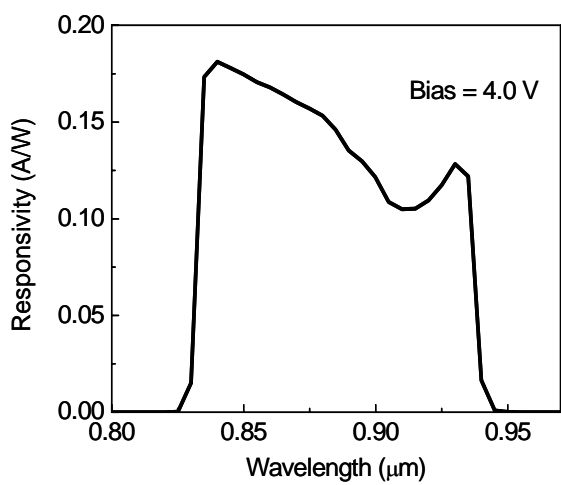
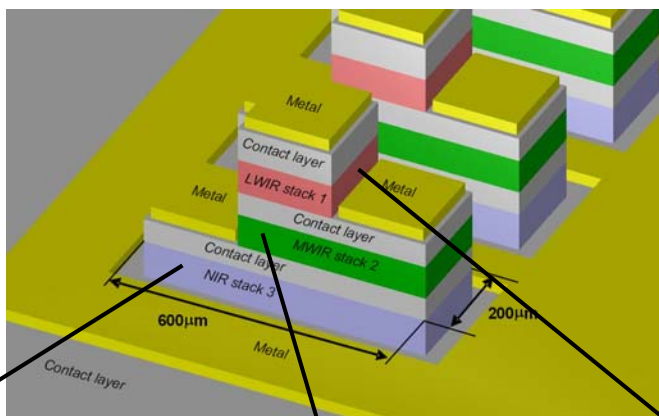
Responsivity Measurements





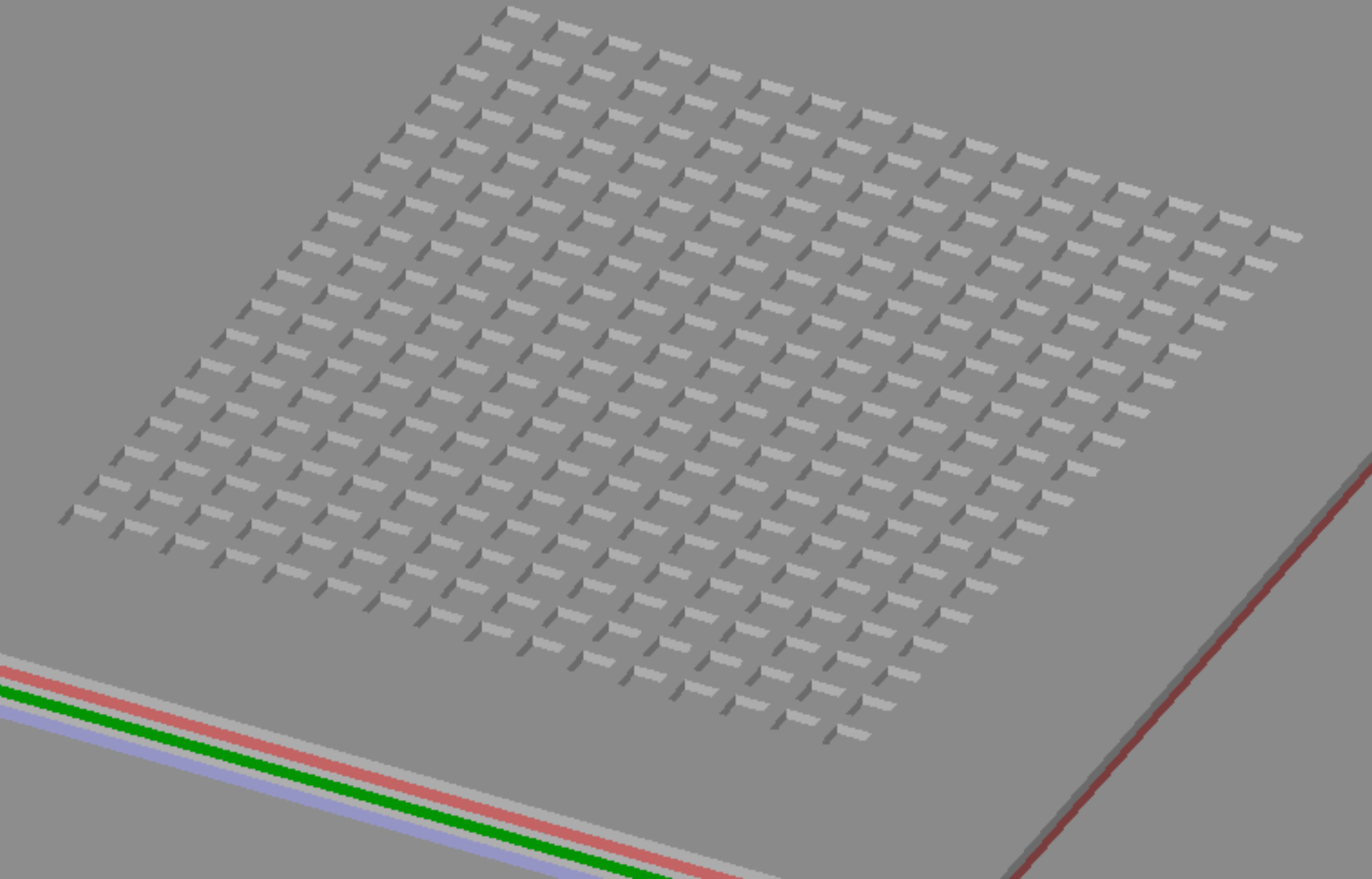
Experimental Results

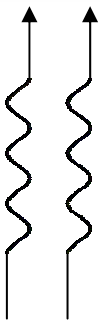
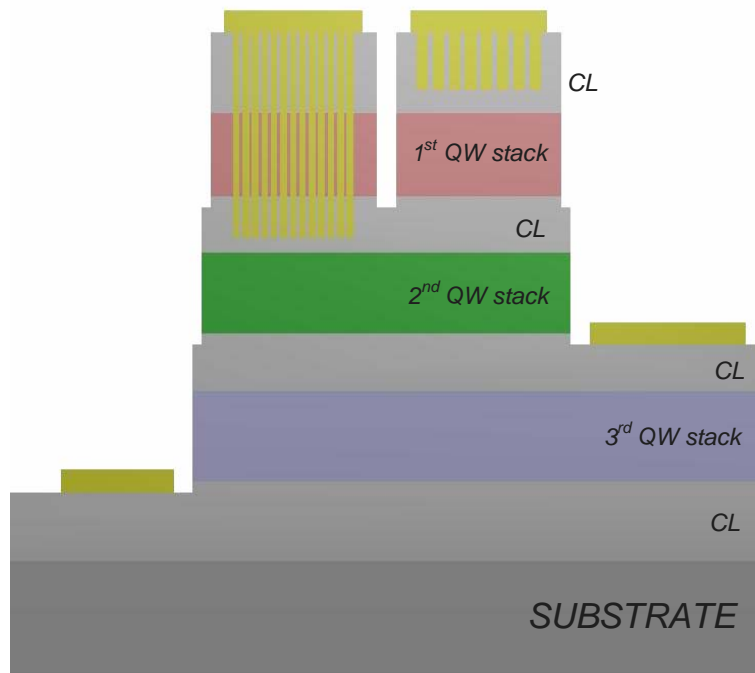
Responsivity Measurements



Future Work

Optical Coupling





Normal incidence detector

Summary

A near-, mid- and long-infrared photodetector with separate readouts was fabricated using interband and intersubband transitions in a quantum well structure.

The measured absorption and photocurrent data show a good agreement with the simplified model develop for the design of the quantum well structure.

The photocurrent spectroscopy measurements demonstrate the possibility of detection of widely separated wavelength bands using interband and intersubband transitions in quantum wells.

Finally, this approach presents a great potentiality in designing detectors to sense specific emission signatures.

***NIR, MWIR and LWIR Quantum Well
Infrared Photodetector using Interband
and Intersubband Transitions***



Fabio Durante P. Alves (ITA – Brazil)



G. Karunasiri and N. Hanson (NPS – USA)



***M. Byloos, H. C. Liu, A. Bezingier
and M. Buchanan (NRC – Canada)***